JOURNAL OF MATERIALS SCIENCE 28 (1993) 1269–1275

Powder compaction interpretation using the power law

M. H. H. ES-SAHEB
Mechanical Engineering Department, College of Engineering, King Saud University, PO Box 800, Riyadh 11421, Saudi Arabia

The effects of strain hardening and axial strain rate, over a wide range of rates (10^{-3} to 10^{5} s^{-1}), on the compaction properties of a variety of pharmaceutical powders have been investigated. The powders tested are: Di Pac sugar, paracetamol d.c., Avicel and lactose. These materials have been assessed using the constants derived from the power law as a criterion to describe their behaviour. All the materials tested show, with varying degrees, a non-linear increase in the yield pressure (flow stress), the constant G, the strain rate exponent m and the strain hardening exponent n as the strain rate increases. These variations are more clear in the materials known to deform plastically, such as Avicel. This is attributable to a change either from ductile to brittle behaviour or a reduction in the amount of plastic deformation due to the time-dependent nature of the plastic flow. This, however, is explained in terms of dislocation and diffusion processes involved in the plastic deformation mechanisms during the compaction process. As the speed of compaction increases the characteristics of deformation, including the value of the strain rate exponent, the shape of the creep curve and the nature of creep rate, suggest that the creep behaviour is therefore controlled by some form of diffusion process. Meanwhile, the creep characteristics of the low and medium rate tests appear to be consistent with dislocation climb and viscous glide. For the materials tested, Avicel is found to be the most strain-rate sensitive material, while paracetamol d.c. is found to be the least strain-rate sensitive material.

1. Introduction

The compaction behaviour of a multi-particulate system is extremely difficult to characterize because there are several discrete mechanisms in operation which overlap and change as compaction proceeds. The initial mechanism involves particle rearrangement and packing down, followed by elastic–plastic deformation and fragmentation, and finally cold-working with or without particle attrition [1].

Initially powder compaction is quantitatively described by pressure–volume relationships, and subsequently by relating compaction pressure to compact properties like hardness and strength. Consequently, from the large quantity of data obtained on both conventional and non-conventional machines, an extensive number of parameters are available for evaluating compaction mechanisms and comparing the compressibility of powders in general, and pharmaceutical powders in particular. Krycer *et al.* [2] have reviewed the most popular methods used and available in the pharmaceutical literature, for interpreting compaction data at low strain rates (i.e. slow speeds). These methods include the use of terms to quantitate the energy required for elastic and plastic deformation, pressure–volume relationships, stress relaxation and elastic recovery measurements, pressure–surface area curves, pressure cycle plots of radial versus axial pressure, etc. Unfortunately none of these methods nor other reported techniques, except very few [3–6], consider systematically the quantitative effect of strain hardening and strain rate in the powder compaction process. Thus, with such a variety of methods available for treating the data, many discrepancies have arisen in the literature: not only among the various techniques, but there are also serious conflicts in the conclusions of researchers employing similar methods. In the author's opinion, that could be mainly due to (i) the strain-rate (i.e. compaction speed) sensitive nature of most pharmaceutical powders, and (ii) the disparity between measuring techniques and working conditions of the different investigators. It is clear from this that there is not any general and conclusive method, relationship or technique, yet, which would characterize the whole process of compaction over the entire ranges of pressures and speeds encountered in this field.

In spite of this complexity, there have been numerous attempts to characterize the compaction process: among these, the early work carried out by Walker [7], Jones [8] and Balshin [9]. Later, in an attempt to allow for all the compaction mechanisms, Donachie and Burr [10] proposed the generalized constitutive equation

$$D = f_1(p) + f_2(p) + f_3(p) + B \quad (1)$$

where D is the current density, $f_1(p)$, $f_2(p)$, $f_3(p)$ are

0022–2461

functions of pressure applying in the first, second and third stages of compaction, respectively, and B is a geometrical constant related to particle size and shape. However, on the whole very little work in determining the forms of the functions $f_1(p)$ and $f_3(p)$ has been carried out. This can be attributed to the fact that, in general, only compacts with densities corresponding to the second stage of the compaction curve are of commercial and practical interest. Meanwhile, Heckel [11] arrived at the constitutive equation

$$\ln\left(\frac{1}{1-D}\right) = KP + A \tag{2}$$

which implies a linear relationship between the pressure P and $\ln[1/(1-D)]$, where D is the density of the compact relative to the absolute density of the material being compacted, K is a constant the reciprocal of which is equal to the mean yield pressure (stress) of the powder, and A is a constant. This equation and rival ones put forward by Kawakita and Tsutsumi [12], and Cooper and Eaton [13] became generally accepted and were widely used in metallurgy, ceramic and pharmaceutical industries.

Although the various equations put forward, especially those of Kawakita and Tsutsumi [12], Heckel [11] and Cooper and Eaton [13] are empirical, they have none the less proved very useful in quantitatively describing the compaction process and allowing comparative experiments to be carried out over a limited range of pressure and compaction speed. But the compaction speed, i.e. the rate of straining of a powder mass, is an important factor affecting its pressure–density behaviour [6]. Hence, it is essential to consider these effects (i.e. the strain hardening and strain rate) to achieve better understanding of the compaction process mechanisms and to gain more accurate information as well as reliable quantitative measures of the powder properties, particularly those powders most sensitive to strain hardening and strain rate properties, over a wide range of pressures and compaction speeds. Thus it is suggested here to employ the more fundamental approach described by the general power law widely used and accepted for describing the creep behaviour in solid metals and alloys [14–17], for interpretation of powder compaction data. The general form of the power law can be given as

$$\sigma = F\varepsilon^n\dot{\varepsilon}^m \tag{3}$$

where σ is the stress (pressure) for an induced strain ε, n the strain hardening exponent, m the strain rate exponent and F a constant. The manipulation of compaction data using this equation was carried out in two steps to elucidate the effects of both, strain hardening and strain rate on the compaction process. These important aspects will be discussed and treated very carefully through this work.

In this paper the use of the power law for evaluating the compaction properties of four pharmaceutical powders is investigated. Thus the strain rate sensitivity as well as the strain hardening characteristics of these materials are evaluated and discussed. The work presented covers a wide range of strain rates ranging from 10^{-3} to 10^5 s^{-1}, for a variety of powders.

2. Experimental procedure

2.1. Materials

The materials investigated in this study (Table I), were chosen because they are among the more commonly used excipients in the pharmaceutical industry, and present all the deformation and bonding mechanisms encountered in the compaction process. The materials were used as received from ICI Pharmaceuticals Division, UK and the respective manufacturers. True densities were determined using an air comparison pycnometer (Beckmann model 930). Five determinations for each material were carried out and the mean value was calculated. For more details of these materials, including results of particle size analysis and electron scanning microscope photographs, see Es-Saheb [18].

2.2. Experimental equipment and techniques

Three different systems (machines), covering the low, medium and high axial strain rates, were employed for compression, to cover a wide strain rate range of 10^{-3} to 10^5 s^{-1}. Cylindrical compacts of 4.1 mm final height from all tested powders were formed on these machines [6, 18, 19].

Compression was carried out firstly by using the ICI hydraulic compression simulator machine [20] fitted with 10 mm flat-faced punches, for the low axial strain rate tests (10^{-3} to 10 s^{-1}). Uniaxial compression was provided by utilizing an "exponential form" displacement–time profile [18] for both upper and lower punches, which produces a constant compression-rate cycle of compaction. The compression rates chosen ranged from 0.0014 to 14 s^{-1}, which

TABLE I The materials investigated

Material	Description	Manufacturer	True density (kg/m^{-3})
Di Pac sugar	Co-crystallization of 97% sucrose and 3% dextrins	Amstar Corp., New York	1580
Paracetamol d.c.	Spray-dried with 4% hydrolysed gelatin	Graesser Salicylates Ltd, Brussels	1270
Avicel enco.	Microcrystalline cellulose	FMC Corp.	1903
Lactose BP	α-monohydrate	Serolac Dairy Crest	1555

encompasses the range encountered during research using physical testing (tablet) machines in industry. Measurements of axial displacement and compaction force were performed using a multi-channel u.v. recorder to an accuracy of $\pm$ 10 μm and $\pm$ 0.025 kN, respectively. To allow true displacement to be determined, the elastic deformations of the punches and other simulator machine parts were evaluated and taken into consideration (i.e. the compacting system rigidity is considered).

For medium (10^2 to 10^3 s^{-1}) and high (10^3 to 10^5 s^{-1}) strain rate tests the compression was carried out using an instrumented drop hammer and a specially designed high-pressure air projectile launcher, respectively [18, 19]. Measurements of axial load and displacement were made and acquired on storage oscilloscopes and processed later.

To allow direct comparison of all materials tested, the weight of each material to give a final relative density of 0.95 was calculated from the true material densities [18]. The actual number of points calculated during each compression cycle was 50. For each material at least three compression tests, were carried out at each compression rate, and the mean values were calculated.

3. Data manipulation and results

In this study Equation 3 together with Equation 2 were used to analyse the relationship among the strain ε, the relative density D, the strain rate $\dot{\varepsilon}$ measured during compaction and the applied pressure P (axial stress σ). These quantities were calculated from the u.v. recorder plots, for low strain rate tests, and the oscilloscope traces, for medium and high strain rate tests [18, 19]. At selected points along the time scale, the deflections of the axial displacement transducers and load cells traces were measured. Having calibrated these transducers and load cells before, it was possible to convert these deflections into force (kN) and displacement (mm), respectively. Knowledge of the punches cross-sectional areas, the initial compact height, the elastic deformation of the punches and the simulator machine (i.e. the machine rigidity), the powder mass and its true density, enables the force to be converted to pressure P (stress σ), and the displacement to strain ε, strain rate $\dot{\varepsilon}$ and the relative density D, to be calculated. However, to calculate the strain hardening exponent n and strain rate sensitivity m, the data were manipulated in two steps. These were as follows.

3.1. Strain hardening effects

As stated above, in order to determine the strain hardening exponent n for the powder, the power law given by Equation 3 is applied at each speed (i.e. strain rate $\dot{\varepsilon}$). However, to be able to employ this law, it is necessary to separate the effect of the strain (ε) and strain hardening from that of the strain rate ($\dot{\varepsilon}$). Thus, for the low strain rate tests (i.e. 10^{-3} to 10 ps^{-1}) where the ICI hydraulic machine is used, as stated above all materials were tested under constant compression rate conditions (i.e. at constant strain rate). Hence it was possible to separate strain rate effects. But for medium and high strain rate tests, where the machines used for compaction engender strain rate effects, it was difficult to achieve the separation. Consequently, the data obtained from these machines were treated as follows. First, for each test the strain rate ($\dot{\varepsilon}$) –time curve is obtained and plotted. Then, from the area under this curve an average mean value for the strain rate ($\dot{\varepsilon}_{av}$) is calculated. This value then (i.e. the average strain rate, $\dot{\varepsilon}_{av}$) is considered to represent the constant compression rate for the test. Therefore, in this case, the power law given by Equation 3 reduces to take the form

$$\sigma = G\varepsilon^n \tag{4}$$

where σ is the axial stress (pressure), ε is the axial strain induced and G is a constant. This constant actually represents the combined value of the terms F and $\dot{\varepsilon}^m$ given by Equation 3, where $\dot{\varepsilon}$ here is actually the constant strain rate value for the low strain rate tests and the average mean value $\dot{\varepsilon}_{av}$ for the medium and high strain rate tests, respectively. Thus, for each test the axial pressure (stress σ) and the axial induced strain ε were calculated as mentioned earlier. These results are plotted on log–log scales and then fitted with the best straight line, the slope of which represents the value of the strain hardening exponent n. The interpolation intercept of this line with the y axis at unit strain represents the value of the constant G (i.e. the stress coefficient of the material). For each rate (i.e. speed) a mean curve is obtained from three compression tests; this is taken as being representative and these curves for all rates tested are plotted on a common axis for each material. Typical examples of this plot for Di Pac sugar powder, compacted in the low strain rate range, are shown in Fig. 1. The variation of the strain hardening exponent n and the constant G with the strain rate for the powders tested are shown in Figs 2 and 3, respectively.

3.2. Strain rate effects

Again after obtaining the values (i.e. the mean) of the constant G and the strain hardening exponent n for each case, and taking these values to be constant at each strain rate (speed) condition, the power law is used once again to manipulate the data to calculate the strain rate exponent m. To achieve this an analogue of the practice used for metals and alloys when applying this law is considered. Thus the power law could be reduced to take the form

$$\bar{\sigma} = Q\dot{\varepsilon}^m \tag{5}$$

where in this case Q is a constant which incorporates the combined effect of the terms F and ε^n given by Equation 3, $\bar{\sigma}$ is the flow stress (pressure), $\dot{\varepsilon}$ is the strain rate (the constant compression rate for the slow tests and the average mean values $\dot{\varepsilon}_{av}$ for the medium and high rate tests, respectively) and m is the strain rate exponent. However, to implement this equation the value of the flow stress has to be evaluated first for each test. However, to determine this value (i.e. the

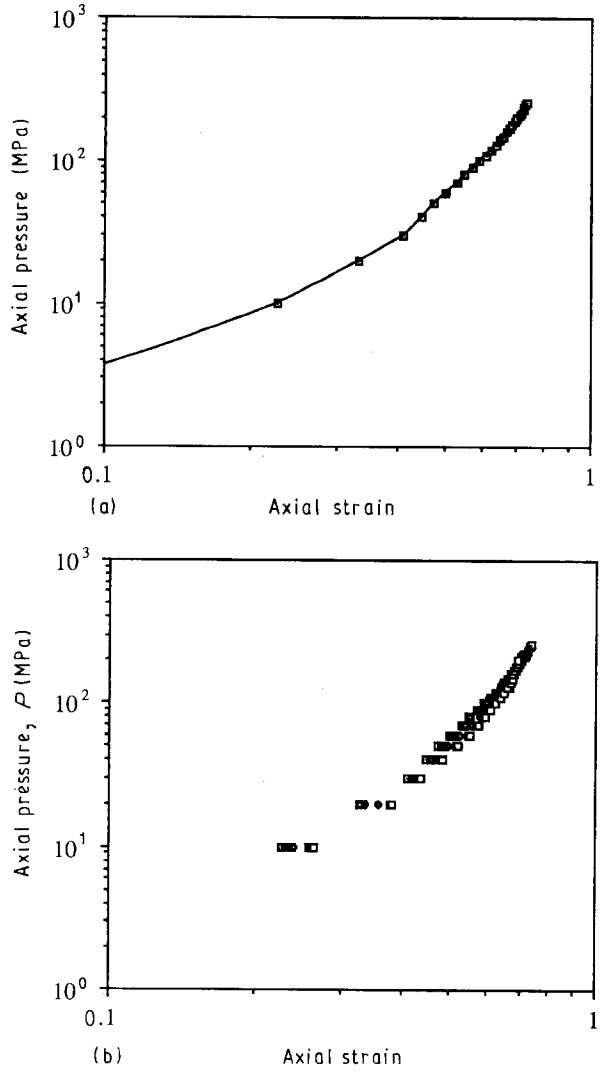

Figure 1 (a, b) Typical axial pressure (σ) versus axial strain (ε) plots for Di Pac sugar powder compacted in the low strain rate range. Strain rate (s^{-1}) : (⊡) 0.0014, (◆) 0.014, (◘) 0.14, (◇) 1.4, (■) 7.0, (□) 14.0.

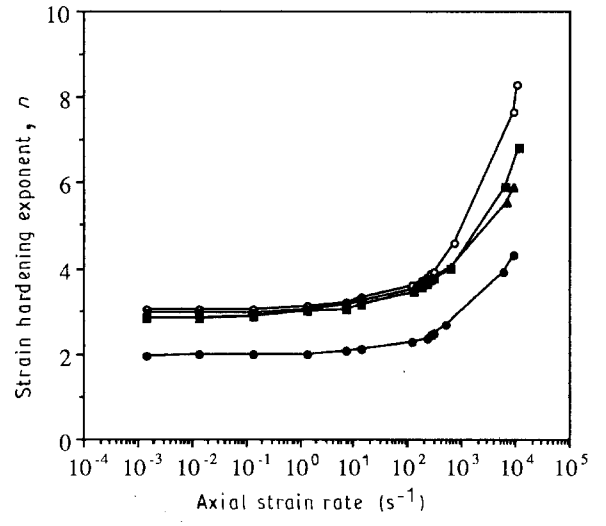

Figure 2 Variation of strain hardening exponent n with axial strain rate $\dot{\varepsilon}$: (■) lactose, (●) Avicel, (○) Di Pac sugar, (▲) paracetamol d.c.

flow stress) for a powder is very difficult, because there is not a single distinct value which would describe the flow stress for all the particles in a powder mass. Thus to overcome this problem, the mean yield pressure

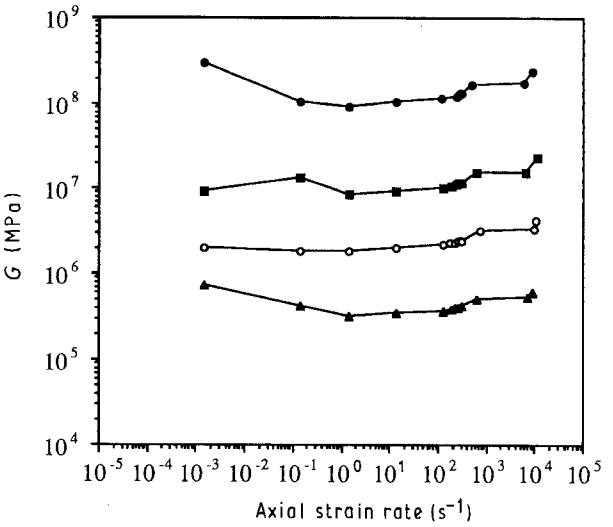

Figure 3 Variation of the constant G with axial strain rate ($\dot{\varepsilon}$) : (■) lactose, (●) Avicel, (○) Di Pac sugar, (▲) paracetamol d.c.

$1/K$ as determined by the Heckel Equation 2 is used to present the flow stress for the powder. Consequently, the values of the axial pressure P and the relative density D for the powders were calculated from the experimental data for each test as described earlier. It was then possible to plot the Heckel curve for each test. However, for each rate (i.e. speed of compaction) a mean curve from three compression tests is taken as being representative, and these curves for all speeds tested are plotted on a common axis for each material. Then, from these Heckel plots, for each case the values of the constant K and its reciprocal (i.e. $1/K$, the mean yield pressure of the powder) are calculated. Typical examples of this plot for lactose powder, compacted in the low and medium strain rate ranges, are shown in Fig. 4. The variations of the mean yield pressure $1/K$ (i.e. the flow stress $\bar{\sigma}$) for the materials examined with the strain rate $\dot{\varepsilon}$ are shown in Fig. 5. Then, by plotting these values of flow stress $\bar{\sigma}$ versus strain rate $\dot{\varepsilon}$ (i.e. the constant strain rates for the low strain rate tests and the actual corresponding average strain rate values $\dot{\varepsilon}_{av}$ for the medium and high strain rate tests) on log–log scales as displayed in Fig. 6, it was possible to obtain the average value of the strain rate exponent m for each material. The variations of the strain rate exponent m over the whole strain rate range for all the materials investigated are shown in Fig. 7.

4. Discussion

In general, it is well known that during the compaction process a non-uniform stress distribution results due to the effect of friction as well as the non-homogeneous nature of the powders. Therefore, the use of the terms stress and strain in this context means the average values rather than the localized ones. This terminology corresponds to the use of the terms pressure and volume changes (i.e. density) usually used in the powder compaction field.

From the plots in Fig. 1 it is clearly seen that for all cases a reasonably linear relation exists over almost the whole tested range of pressures and speeds of compaction for all the materials. This means that

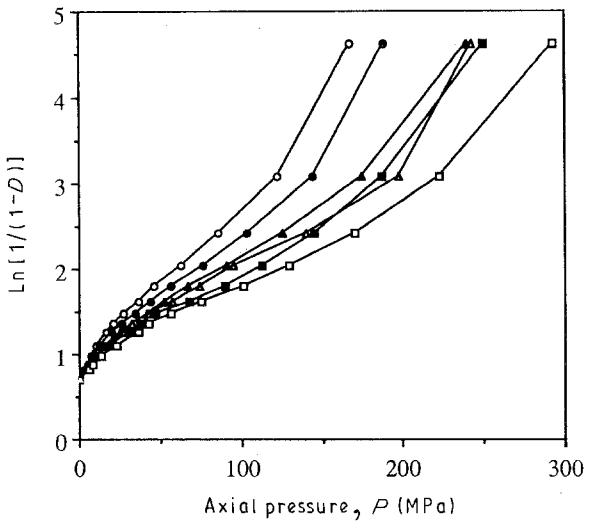

Figure 4 Typical Heckel plots for lactose powder compacted at low and medium strain rates. Strain rate (s^{-1}): (○) 0.0014, (●) 0.14, (▲) 14, (△) 125, (■) 270, (□) 310.

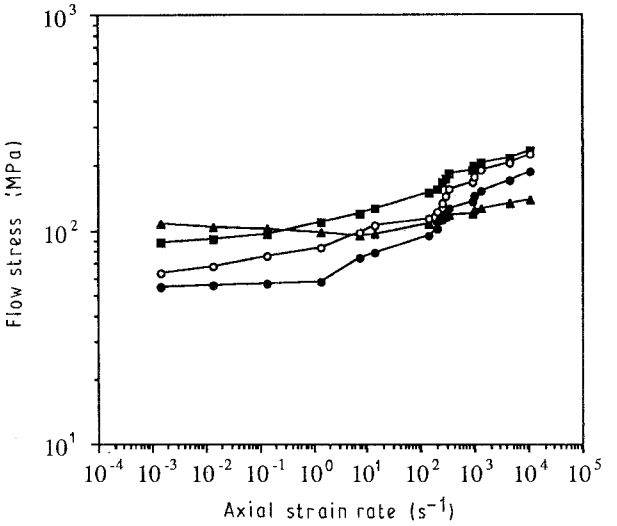

Figure 6 Variation of flow stress $\bar{\sigma}$ with axial strain rate $\dot{\varepsilon}$: (■) lactose, (●) Avicel, (○) Di Pac sugar, (▲) paracetamol d.c.

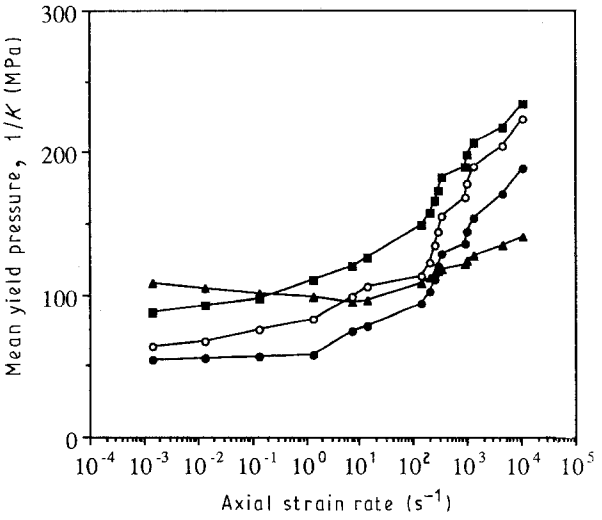

Figure 5 Variation of mean yield pressure $1/K$ with axial strain rate $\dot{\varepsilon}$: (■) lactose, (●) Avicel, (○) Di Pac sugar, (▲) paracetamol d.c.

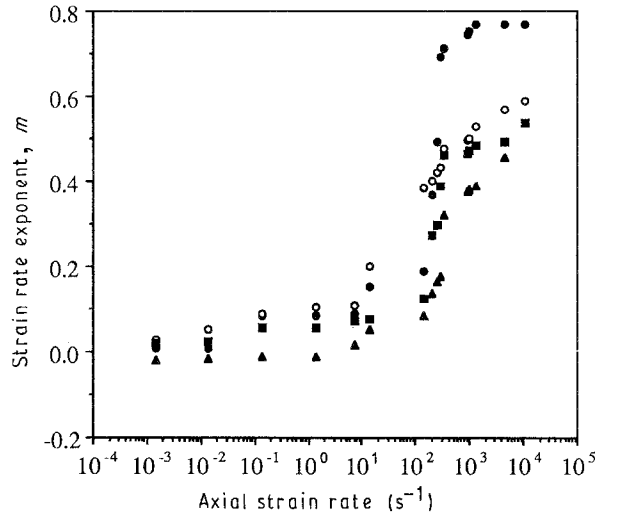

Figure 7 Variation of strain rate exponent m with axial strain rate $\dot{\varepsilon}$: (■) lactose, (●) Avicel, (○) Di Pac sugar, (▲) paracetamol d.c.

more reliable values of the constants G and n can be obtained. Since these constants are believed to describe the effect of the initial material conditions, the material behaviour and the deformation mechanisms, they could be used, in a similar manner to the Heckel equation constants, in characterizing the powder behaviour and its various deformation mechanisms during compaction.

It is noticed that as the speed of compaction increases, so does the value of n (i.e. the strain hardening exponent) for all powders tested (see Fig. 2). Meanwhile the value of the constant G is slightly increased as shown in Fig. 3. The small change in the values of G could be due to the different starting initial conditions as a result of the small weight differences, as well as the different particle size and shape distribution of the material in each case. This would affect the initial density of the compacted material and hence the constant G. Also, due to the effect of compaction speed on the various deformation mechanisms, particularly the type of dislocation and diffusion mechanisms involved at each speed, the values of the strain hardening exponent n are affected. This is clearly shown in Fig. 2. At higher speeds the powder tends to behave in a more brittle fashion and the actual plastic deformation becomes less, giving higher values of n.

It has been implied that the parameters G and n are material constants but one cannot, for example, assume that the magnitude of these parameters is fixed for a material whose structure can be significantly altered by the speed and pressure of compaction. In effect, each chemical composition and condition of microstructure must be viewed as a different material as far as G and n are concerned. What must be realized, however, is that the values of the parameters should be determined with specimens that contain no effect of work-hardening prior to the compression deformation itself. After all, G and n are the very parameters used to describe the work-hardening characteristics. Hence the values of these constants are found to be indicative of the material properties and behaviour including its morphology and chemical structure. For example, the value of G is relatively higher for plastic "amorphous" material and low

speeds of compaction, while for brittle crystalline materials and relatively higher speeds it becomes lower. This is contrary to the change in values of n, i.e. higher values for brittle behaving materials and higher speeds, and lower values for plastic behaviour of materials and lower speeds. This can be clearly seen from the values of G and n for the plastic amorphous Avicel where G is relatively high and n low, and the brittle and crystalline paracetamol d.c. where G is relatively low and n is high. It must be considered, however, that the speed of compaction is always affecting the material behaviour and hence the changes in the values of G and n.

Furthermore, the significance of these constants could be related to the "capping" tendency in the various powders in each case. It is noticed that when the value of G is high and n is low the capping tendency in certain materials is reduced (e.g. Avicel powder), while if the value of G is low and n is high a capping tendency of the material is more likely (e.g. paracetamol d.c. powder). It is also noticed that, almost in all cases, the higher the value of $1/K$ (the mean yield pressure obtained from a Heckel plot) the higher is the value of n and the lower is the value of G, while lower $1/K$ values coincide with lower n and higher G values.

The combined effects of all deformation mechanisms involved in the process of compaction are very much affected by the speed of compaction, particularly the ductile and brittle behaviours of the powder [18], and consequently the form of the compaction curves. This is clearly shown in the plots of Fig. 4. However, at the higher strain rates and strains, non-linear behaviour is noticed. This is believed to be due to the increasingly brittle behaviour of the various materials in this range of speeds and strains [5] as well as the cold-working of the compact. This, however, differs from one powder to another depending on its mechanical properties and behaviour under the various loading conditions. As expected, all the materials tested exhibit compression rate effects to some extent.

For all materials non-linearity is observed in the Heckel plots over the whole compaction pressure and speed ranges studied (see Fig. 4). This indicates that none of the materials examined deform exclusively by a plastic deformation mechanism, including the powders which are known to deform plastically such as Avicel. It is noticed also that as the speed of compaction increases the non-linearity of the plots increases. This indicates that a fragmentation mechanism becomes increasingly dominant and the material tends to become more brittle, hence the increasing non-linearity of the Heckel plots and higher values of the mean yield pressure $1/K$.

This non-linear behaviour in all the Heckel plots obtained makes it very difficult to determine the exact value of the mean yield pressure $1/K$. However, to overcome this problem, for each case the slope values of up to 30 points on the plot over the second stage of compaction (where the slope value change is very small, about $\pm$ 0.3%) are obtained. Then the average slope value is calculated, the reciprocal of which is taken to be equal to $1/K$ (i.e. the flow stress).

It is found that the descending order of materials tested regarding their plastic deformation behaviour as shown in Figs 5 and 6 is Avicel, Di Pac sugar, lactose, paracetamol d.c.

As far as the compaction rate (speed) is concerned, Rue and Rees [21] found that with an increased contact time, i.e. slow speeds, they obtained a greater consolidation, but this is material-dependent. A large change in consolidation with changing contact time is indicative of plastically deforming dominant material. This is in perfect agreement with our findings, as can clearly be seen from the values of $1/K$ obtained for the same powder at the various speeds of compaction and shown in Figs 5 and 6. It is noticed also that the variation of the mean yield pressure (i.e. the flow stress) with the axial strain rate starts almost linear at very low speeds of compaction, where the plastic deformation mechanism is believed to be dominant and becomes increasingly non-linear as the speed increases.

Rate effects are important, particularly when one wishes to predict compaction loads at strain rates which may be as high as 10^5 s^{-1} from data obtained in a laboratory compression test in which the strain rates may be as low as 10^{-4} s^{-1}; the flow stress should be corrected unless m is very small. It is known that strain rate sensitivity is also temperature-dependent. Again it is important here to mention that, although the definition of m in the literature is usually based upon shear stress and strain rate, it is equivalent to the definition derived from Equation 5.

In the second stage of compaction, differences between quasi-static and dynamic compaction behaviour suggest that the yield strength of the powder must vary with the rate of compaction (see Fig. 5). Numerous workers in solid mechanics have found that the flow stress of solids increases as the rate of deformation is increased. The variation in flow stress with deformation rate (see Fig 6) is usually explained in terms of dislocation movement and interaction [22].

For the materials tested and many other metallic alloys [16] there is a minimum in m near room temperature and low strain rates and, as indicated, negative m values are sometimes found, (see Fig. 7). At low strain rates, as in metallic alloys, solutes (particularly in the case of non-homogeneous composite powders and mixtures such as paracetamol d.c. [5]) segregate to dislocations; this lowers their energy so that the forces required to move the dislocations are higher than those required for solute-free dislocations (i.e. the mono-powders). At increased strain rates, however, dislocations move faster than solute atoms can diffuse [16], so the dislocations are relatively solute-free and the drag is minimized. A negative rate sensitivity tends to localize flow in a narrow region which propagates along the compacted specimen as a band, (see Fig. 7) where negative values of m are observed (e.g. paracetamol d.c. powder). This, also, could be attributable to variation of the plastic deformation taking place within the powder mass during compaction as a result of the changing frictional effects. By localization of flow in a narrow band, the deforming material experiences a higher strain rate

and therefore a lower flow stress. The higher values of rate sensitivity are attributed to the increased rate of thermally activated processes such as dislocation climb and grain boundary sliding.

From Fig. 6 (which shows the dependence of flow stress for all materials tested upon strain rate) and Fig. 7 (which shows the corresponding values of m as a function of strain rate) it is clear that at the higher strain rates, m is typical of thermally activated slip. Meanwhile, at lower strain rates, deformation mechanisms other than slip prevail. Here there are two schools of thought [16]. One maintains that deformation occurs primarily by diffusional creep with vacancies migrating from grain boundaries parallel to the compression axis to those normal to it. This diffusion causes the grains to contract in the compression direction and to elongate laterally. Whether diffusion is through the lattice or along grain-boundary paths, the strain rate should be proportional to the applied stress and inversely related to the grain size. If diffusion were the only mechanism, m would equal one (Newtonian viscosity) but it is lowered because of the slip contribution to the overall strain. The other school attributes the high rate sensitivity to the role of grain-boundary sliding (shearing on grain boundaries). Although grain-boundary sliding alone would be viscous ($m = 1$), it must be accompanied by another mechanism to accommodate compatibility at triple points where the grains meet. Either slip or diffusion could serve as the accommodating mechanism. Both models explain the need for using very fine grain-size materials and low strain rates.

It is clear from Fig. 7 also that the strain rate exponent m, for all the tested powders, varies in its value with the range of strain rate, resembling linear behaviour at low speeds (where the glide mechanism is responsible for plastic deformation) and a non-linear trend at higher rates (where the climb mechanism and diffusion are dominant).

5. Conclusion

In the powder compaction process, the combined effects of mechanical deformation mechanisms, the morphology and the chemical structure of the powder as well as the speed of compaction (strain rate) are incorporated and could be described by the parameters G, n (the strain hardening exponent) and m (the strain rate exponent) obtained by employing the power law, for each case. The variation of these characteristic parameters with the strain rate is found to be non-linear. The values of G, n and m as well as the flow stress are found to increase as the strain rate increases. Dislocation mechanisms (slip, glide, climb etc.) are believed to be dominant during plastic deformation at low speeds. On the other hand, at higher speeds (strain rates) some form of diffusion mechanism tends to be dominant during the compaction process.

References

1. R. P. SEELING and J. WULFF, *Trans. Amer. Inst. Mining Met. Engrs.* **166** (1946) 492.
2. I. KRYCER, D. G. POPE and J. A. HERSEY, *Drug Develop. Ind. Pharmacy* **8** (3) (1982) 307.
3. S. T. DAVID and L. L. AUGSBURGER *J. Pharm. Sci.* **66** (1977) 155.
4. D. BARTON, MSc dissertation, University of Manchester (1978).
5. S. T. S. Al-HASSANI and M. ES-SAHEB, in proceedings of 3rd Oxford Conference on the High Strain Rate Properties of Materials, Oxford, UK, April 1984, p. 421. (The Institute of Physics, London, 1984).
6. M. ES-SAHEB, M. A. SARUMI and S. T. S. Al-HASSANI, in Proceedings of World Conference on Powder Metallurgy P/M 90, London, UK July, 1990, Vol. 1, p. 533.
7. E. E. WALKER, *Trans. Faraday Soc.* **19** (1923) 73.
8. W. D. JONES, "Principle of Powder Metallurgy" (Arnold, London, 1937) pp. 3–27.
9. M. Y. BALSHIN, *Vestnik Metalloprom* **18** (2) (1938) 124 (Russian Translation Programme RTS 6335).
10. M. J. DONACHIE and M. F. BURR, *J. Metals* **15** (1963) 849.
11. R. W. HECKEL, *Trans. Metall. Soc. AIME* **221** (1961) 671.
12. K. KAWAKITA and Y. TSUTSUMI, *Bull. Chem. Soc. Jpn* **39** (1966) 1364.
13. A. R. COOPER Jr and L. E. EATON, *J. Amer. Ceram. Soc.* **45** (1) (1962) 97.
14. W. R. CANNON and O. D. SHERBY, *Metall. Trans. A.* **1** (1970) 1030.
15. M. S. SOLIMAN and F. A. MOHAMED, *ibid.* **15** (1984) 1893.
16. M. S. SOLIMAN, *J. Mater. Sci.* **22** (1987) 3529.
17. W. F. HASFORD and R. M. CADDELL, "Metal Forming Mechanics and Metallurgy" (Prentice Hall, Englewood Cliffs, NJ, 1983) p. 49.
18. M. H. H. ES-SAHEB, PhD thesis, University of Manchester (1985).
19. *Idem, J. Mater. Sci.* **27** (1992) 4151.
20. B. M. HUNTER, D. G. FISHER, P. M. PRATT and R. C. ROWE, *J. Pharm. Pharmac.* **28** (1976) Suppl. 65P.
21. P. R. RUE and J. E. REES, *ibid.* **30** (1978) 601.
22. J. D. CAMPBELL, *Mater. Sci. Engng* **12** (1973) 3.

Received 1 November 1991
and accepted 9 July 1992